Polymer 51 (2010) 4249–4258

Contents lists available at ScienceDirect

Polymer

journal homepage: www.elsevier.com/locate/polymer

Order–order, lattice disordering, and order–disorder transition in SEBS studied by two-dimensional correlation infrared spectroscopy

Tao Zhou [a,*], Zhiyong Wu [b], Yunyong Li [a], Jiang Luo [a], Zhengguang Chen [a], Jingkui Xia [b], Hongwen Liang [b], Aiming Zhang [a,*]

[a] State Key Laboratory of Polymer Materials Engineering of China, Polymer Research Institute, Sichuan University, Chengdu 610065, China
[b] Baling Petrochemical Industry Co., Ltd of China Sinopec, Yueyang 414014, China

ARTICLE INFO

Article history:
Received 7 March 2010
Received in revised form
17 May 2010
Accepted 30 June 2010
Available online 7 July 2010

Keywords:
SEBS
Two-dimensional correlation infrared spectroscopy
Transition

ABSTRACT

The temperature-dependent transitions of polystyrene-*block*-poly(ethylene-*co*-1-butene)-*block*-polystyrene block copolymer (SEBS) at high temperature were studied using infrared spectroscopy combined with two-dimensional (2D) correlation spectroscopy. The order–order transition (OOT), the lattice disordering transition (LDT), and the order–disorder transition (ODT) of SEBS were explored with a linear temperature increment ranging from 100 to 220 °C. AFM was employed to study the surface morphology of SEBS and to identify the correlation intensity peaks in the MW2D spectra. The OOT was determined around 152 °C. The LDT appears around 170 °C. The ODT was also successfully determined around 202 °C. It is gained that the key driver of the OOT is the movements of $-CH_2-$ in the main chains of EB blocks. In the LDT, the movements of groups are simultaneous and the SEBS molecular chains move as a whole. In the ODT, it shows the driver is the movements of $-CH_2-$ in the main chains of EB blocks.

1. Introduction

Block copolymers can form various types of separated microphase structures, which range from gyroid, lamellae, cylinders to spheres depending on the content of the constituent blocks and the difference of solubility parameters [1–8]. Many studies have been reported that block copolymers presented several morphological transitions with the temperature increments [9–12]. The transition from one ordered microstructure to another and the transition from one ordered state to microdomains disappearing are referred as the order–order transition (OOT) and the order–disorder transition (ODT), respectively [13–21]. For highly asymmetric block copolymers, there exists the lattice disordering transition (LDT) [22–26], which is defined as the transition from the spheres in a body-centered cubic (BCC) lattice to the disordered spheres.

Polystyrene-*block*-poly(ethylene-*co*-1-butene)-*block*-polystyrene block copolymer (SEBS) is one of the earliest industrial thermoplastic elastomers [1,27]. Fig. 1 shows a molecular structure of SEBS, which has polystyrene (hard block S) at both ends and poly(ethylene-*co*-1-butene) (soft block EB) in the middle. Like other block copolymers, SEBS displays various separated microphase structures with the S blocks (or EB blocks) volume ratio and other conditions changing [1,27–30].

The OOT, LDT, and ODT of SEBS were studied by several research groups [26,31–33]. According to the literature [26,31–33], the experimental methods to determine the OOT, LDT, and the ODT were small-angle X-ray scattering (SAXS), small-angle neutron scattering (SANS), rheological measurements, differential scanning calorimetry measurement (DSC), and transmission electron microscopy (TEM). Most of these studies on these systems focused on the morphological changing, the pathway, and the kinetics of the OOT, LDT, or the ODT. Recently, we have investigated the temperature-dependent molecular chain movements and transitions of SEBS with the moving-window two-dimensional correlation infrared spectroscopy (MW2D) [34]. We found MW2D was a powerful method to clarify temperature-dependent transitions of block copolymers.

To determine the phase-transition temperatures of a thermotropic liquid crystal sample, moving-window two-dimensional correlation spectroscopy method was introduced by Thomas and Richardson [35]. This method was an extension of generalized two-dimensional correlation spectroscopy [36–44], proposed by Noda [45]. MW2D can be direct applied to view spectral correlation variation along both spectral variables (e.g., wavenumber) and perturbation variables (e.g., temperature) axis [46–49]. Therefore, from the correlation intensity along the perturbation variables direction the transition point can be determined. Recently, several

* Corresponding authors. Tel.: +86 28 85405868; fax: +86 28 85402465.
E-mail addresses: zhoutaopoly@scu.edu.cn (T. Zhou), amzhang215@vip.sina.com (A. Zhang).

0032-3861/$ – see front matter © 2010 Elsevier Ltd. All rights reserved.
doi:10.1016/j.polymer.2010.06.051

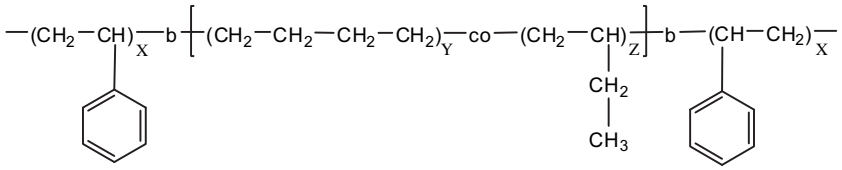

Fig. 1. Molecular structure of SEBS. X and $Y + Z$ represent the polymerization degrees of the hard and soft blocks of SEBS, respectively.

researchers have reported the successful applications of MW2D, which can easily be applied to determine the glass transition, the melting point, and the phase-transition point of polymers [46,49–55].

In this paper, the OOT, LDT, and the ODT of SEBS were studied with infrared spectroscopy combined with two-dimensional correlation analysis. The atomic force microscopy (AFM) measurement was also employed to aid the determination from the MW2D correlation spectra. The OOT, LDT, and the ODT were determined at 152 °C, 170 °C, and 202 °C, respectively.

2. Experimental section

2.1. Materials

Commercial SEBS G1657, a highly asymmetric block copolymer, was used in the experiment. It was bought from Shell Development Co and contains roughly 30 wt% diblock copolymer. The weight-average molecular weight of G1657 is 70,000 g/mol and its polydispersity index ($\overline{M}_w/\overline{M}_n$) is 1.05. Because the soft/hard ratio is 87/13 (wt), the G1657 is expected to form a body-centered cubic (BCC) sphere morphology.

2.2. FTIR spectroscopy

SEBS was spread on one side of a KBr disk by solvent casting from 40 g/L cyclohexane solution. The KBr disk (0.8 mm thick), with the SEBS film sample, was dried in a vacuum oven at 90 °C for 240 min with a −0.08 MPa vacuum degree. The SEBS film disk sample was placed in a homemade temperature control instrument including program heating cell and circulation water jacket cooling system. The temperature-dependent absorbance IR spectra in the 4000–400 cm^{-1} region were measured with Bruker Tensor 27 FTIR spectrometer, equipped with a deuterated l-α-alaninedoped triglycine sulfate (DLaTGS) detector. The spectral resolution was 4 cm^{-1} and the number of the scans of each spectrum was 20. The SEBS film disk sample was heated from 20 °C to 90 °C at a constant rate of 5 °C/min. The temperature was keep at 90 °C for 5 min and continued to increase from 90 °C to 220 °C. Sixty IR spectra were collected from 100 °C to 220 °C (5 °C/min increasing rate) at approximately 2 °C increments. The SEBS film sample was protected by dried high-purity nitrogen gas during the measurement.

2.3. AFM measurement

The atomic force microscopy (AFM) was employed to explore the surface morphology of SEBS (G1657). The SEBS film samples on mica flakes (Φ15 mm) in AFM experiment were cast from 40 g/L cyclohexane solution and their thickness was 1–2 μm. The mica flakes, with the SEBS film samples, were dried in a vacuum oven at 90 °C for 240 min with a vacuum degree of −0.08 MPa. After cooled down to 20 °C, the SEBS film samples were placed in a small homemade vacuum oven (−0.09 MPa). It is specially designed and the temperature can be controlled within 1 °C. We prepared 4 samples for AFM experiments through the method described below: each sample was heated from 20 °C to 90 °C at a constant rate of 5 °C/min. Then the temperature was keep at 90 °C for 5 min and continued to increase from 90 °C to 140 °C (sample **1**), from 90 °C to 152 °C (sample **2**), from 90 °C to 170 °C (sample **3**), from 90 °C to 202 °C (sample **4**), respectively. And then the sample was kept at the destination temperature for 5 min and rapid quenched with freezing absolute ethyl alcohol (−18 °C). Tapping-mode AFM images were gained under normal conditions in air using a Nano-Scope III Multimode AFM (Digital Instruments). A silicon tip was used with 1.0 Hz scan rate.

2.4. Two-dimensional correlation analysis

In this study, all the MW2D and generalized 2D correlation spectra were processed and calculated using two-dimensional correlation spectroscopy software, 2DCS (version 4.3), developed by one of the authors (Tao Zhou). Before performing the analysis, the intensity of each IR spectrum was normalized. The normalized intensity at the given wavenmbers was calculated according to the following equation:

$$A(v) = \frac{I(v)}{\frac{1}{N}\sum_{i=1}^{N} I(v_i)} \quad (1)$$

where $A(v)$ is the normalized intensity and $I(v)$ is the original intensity. Parameter v is the spectral variable (e.g. wavenumbers). Parameter i is the index of data points in an infrared spectrum. Here, the region of the spectral variable is 4000–400 cm^{-1}.

During the calculation, the window size was chosen as $2m + 1 = 11$ to produce the MW2D correlation IR spectra with high quality. The 5% autocorrelation intensity of MW2D correlation spectra was regarded as noise and was cut off. Of special attention is the MW2D correlation spectra were calculated from the whole IR spectral region (4000–400 cm^{-1}) of SEBS. In the generalized 2D correlation spectra and the MW2D spectra, red and blue areas represent the positive and negative correlations, respectively. It should be noticed that the small crosses in the generalized 2D correlation spectra are used to mark the precise position between two wavenumbers. These crosses are not the positive sign.

Table 1
The bands assignments of SEBS IR spectra.

Wavenumber (cm^{-1})	Assignments	
	EB block	S block
2962	C–H asymmetry stretching, $-CH_3$	–
2923	C–H asymmetry stretching, $-CH_2-$	C–H asymmetry stretching of main chain, $-CH_2-$
2852	C–H symmetry stretching, $-CH_2-$	C–H symmetry stretching of main chain, $-CH_2-$
763	–	=C–H bending vibration of side benzene ring
721	C–H Rocking, $-CH_2-$	–
702	–	=C–H bending vibration of side benzene ring

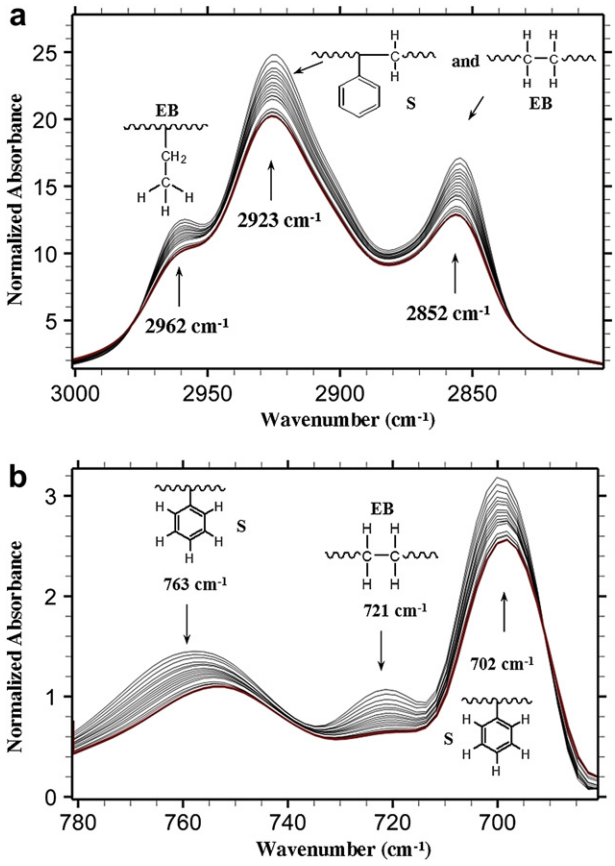

Fig. 2. Normalized temperature-dependent IR spectra of SEBS (100–220 °C). The red spectrum curve is the last collected spectrum (at 220 °C). Key: (a) 3000–2800 cm^{-1}; (b) 780–680 cm^{-1}. (For interpretation of the references to colour in this figure legend, the reader is referred to the web version of this article.)

3. Theory

The theory of MW2D and generalized 2D correlation spectroscopy has been described before [34,37,45]. The algorithm of MW2D correlation spectroscopy also has been described in the literature [34,46]. It is easy to develop a computer program of MW2D using C, C++, FORTRAN, or Perl computer languages.

4. Results and discussions

4.1. The IR spectrum of SEBS

The IR spectrum of SEBS is the overlapping of the S blocks (atactic polystyrene) and the EB blocks (poly(ethylene-*co*-1-butene)). The bands assignments of SEBS spectra are summarized in Table 1 [56–61].

Fig. 2 shows the normalized temperature-dependent (100–220 °C) IR spectra of SEBS. For clarity, the whole spectra are not shown. The red spectrum curve is the last spectrum collected (at 220 °C). As shown in Fig. 2(a), the peak at 2962 cm^{-1} is assigned to the C–H asymmetry stretching vibration of $-CH_3$ of ethyl branches of EB blocks. The peaks at 2923 cm^{-1} and 2852 cm^{-1} are assigned to the C–H asymmetry and symmetry stretching vibration of the $-CH_2-$ in the main chains of the EB and S blocks, respectively. In Fig. 2(b), the peaks at 702 cm^{-1} and 763 cm^{-1} are assigned to the =C–H bending vibration of the side benzene ring of the S blocks. The peak at 763 cm^{-1} shifts to lower wavenumbers and the intensity of 702 cm^{-1} decreases as the temperature increases. The peak at 721 cm^{-1}, assigned to the $-CH_2-$ rocking vibration of the EB blocks, dramatically disappears at 220 °C. Although the gradual variations are noted in the temperature-dependent IR spectra, useful information about the transitions cannot be gained.

Fig. 3 shows the MW2D correlation spectra based on autocorrelation calculations in the 3000–2800 cm^{-1} and 780–680 cm^{-1} region. Around 118 °C, three positive correlation intensity peaks are observed. It is an outcome of the S block glass transition which has been reported in our previous study [34]. The temperature, around 140 °C, has also been reported in our previous paper [34]. It can be explained as the polystyrene main chains of the S block center starting to move entirely. Thus, this temperature corresponds to the

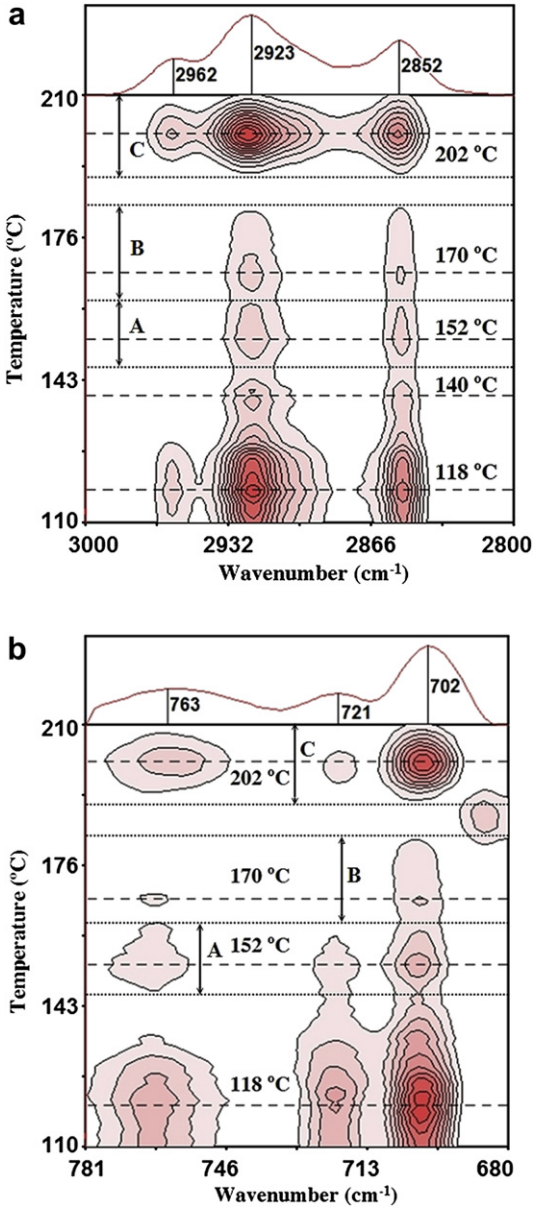

Fig. 3. MW2D correlation spectra based on autocorrelation calculated from the temperature-dependent IR spectra of SEBS (100–220 °C). The contour levels represent the projection of MW2D correlation intensity. The horizontal dashed lines correspond to the temperature point at 118 °C, 140 °C, 152 °C, 170 °C, and 202 °C, respectively. A, B, and C are the defined temperature range of the OOT, LDT, and ODT. Key: (a) 3000–2800 cm^{-1}; (b) 780–680 cm^{-1}.

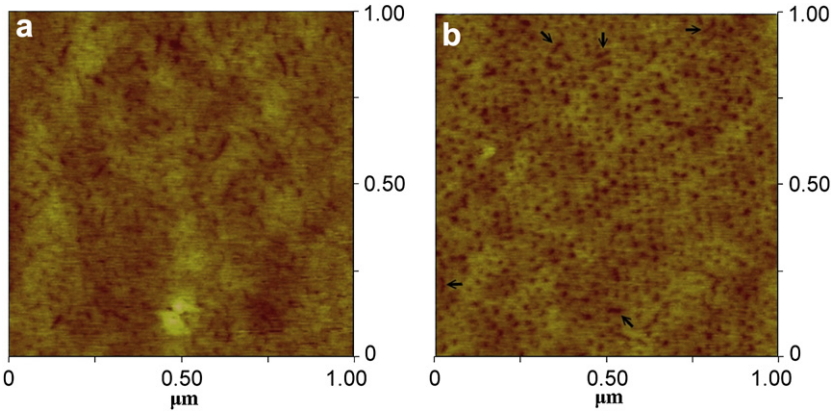

Fig. 4. AFM height images (1 × 1 μm) showing the surface morphology of SEBS films on mica flakes. Key: (a) sample **1**, prepared through rapid quenching with freezing absolute ethyl alcohol at 140 °C; (b) sample **2**, prepared through rapid quenching with freezing absolute ethyl alcohol at 152 °C. The small arrows show the position of some PS "worm".

viscous flow temperature of the main chains of the S blocks. As discussed above, the results of our previous study agree with that of this experiment and calculations.

4.2. Order–order transition

As shown in Fig. 3, several correlation intensity peaks around 152 °C are viewed, except at 2962 cm^{-1}. Krishnamoorti et al. [31–33] reported the "worm like" cylinder-to-sphere order–order transition (OOT) of SEBS was within 135–141 °C. However, in the present study, if the OOT occurs around 140 °C, due to the chemical joint and the interface between EB and S blocks [34], the movement of the S block molecular chains certainly involves a fraction of the EB blocks. In fact, we can just find two correlation intensity peaks (around 140 °C, Fig. 3) at 2923 cm^{-1} and 2852 cm^{-1} which are assigned to the movement of the $-CH_2-$ of main chains in PS. Thus,

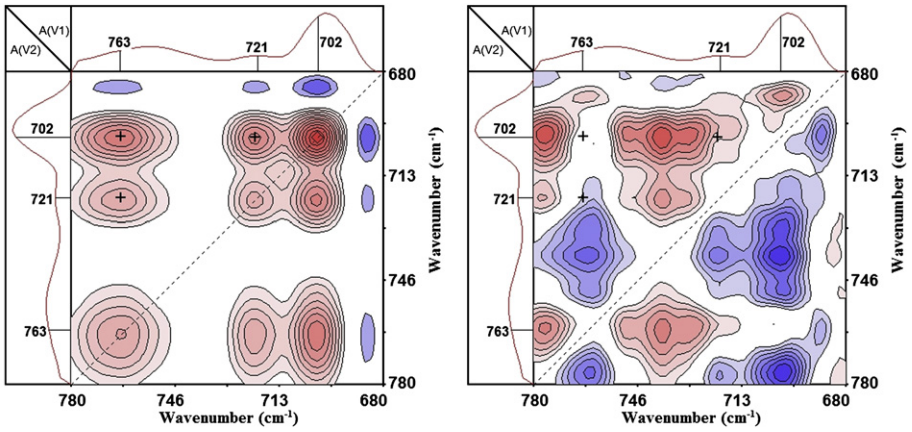

Fig. 5. Synchronous and asynchronous IR spectra of the OOT (145–164 °C) in 780–680 cm^{-1}. The small crosses mark the precise position at (763 cm^{-1}, 702 cm^{-1}), (721 cm^{-1}, 702 cm^{-1}), and (763 cm^{-1}, 721 cm^{-1}). Red and blue areas represent positive and negative correlations, respectively. (For interpretation of the references to colour in this figure legend, the reader is referred to the web version of this article.)

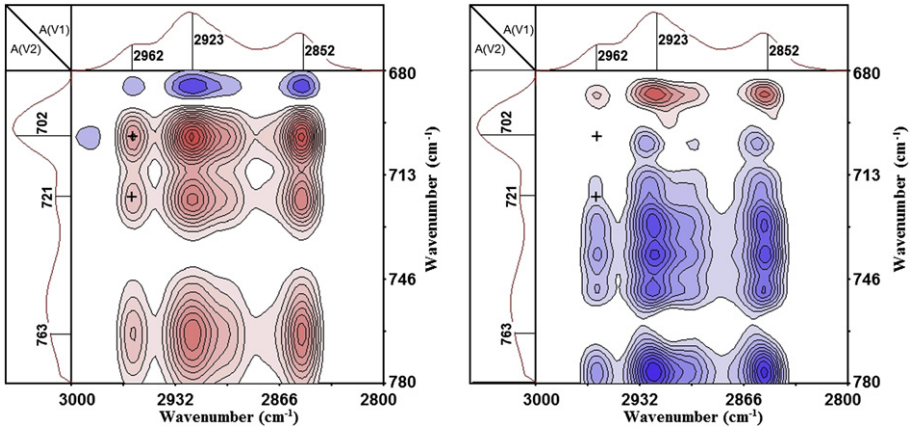

Fig. 6. Synchronous and asynchronous IR spectra of the OOT (145–164 °C) between 780–680 cm^{-1} and 3000–2800 cm^{-1}. The small crosses mark the precise position at (2962 cm^{-1}, 702 cm^{-1}) and (2962 cm^{-1}, 721 cm^{-1}).

Table 2
The results of the generalized 2D correlation analysis in the OOT, LDT, and ODT.

Transitions	Synchronous (Φ)	Asynchronous (Ψ)	Sequential order
OOT	($763\ cm^{-1}$, $702\ cm^{-1}$) > 0	($763\ cm^{-1}$, $702\ cm^{-1}$) = 0	$763\ cm^{-1} = 702\ cm^{-1}$
	($721\ cm^{-1}$, $702\ cm^{-1}$) > 0	($721\ cm^{-1}$, $702\ cm^{-1}$) > 0	$721\ cm^{-1} \rightarrow 702\ cm^{-1}$
	($763\ cm^{-1}$, $721\ cm^{-1}$) > 0	($763\ cm^{-1}$, $721\ cm^{-1}$) < 0	$763\ cm^{-1} \leftarrow 721\ cm^{-1}$
	($2962\ cm^{-1}$, $702\ cm^{-1}$) > 0	($2962\ cm^{-1}$, $702\ cm^{-1}$) = 0	$2962\ cm^{-1} = 702\ cm^{-1}$
	($2962\ cm^{-1}$, $721\ cm^{-1}$) > 0	($2962\ cm^{-1}$, $721\ cm^{-1}$) < 0	$2962\ cm^{-1} \leftarrow 721\ cm^{-1}$
LDT	($763\ cm^{-1}$, $702\ cm^{-1}$) > 0	($763\ cm^{-1}$, $702\ cm^{-1}$) = 0	$763\ cm^{-1} = 702\ cm^{-1}$
	($721\ cm^{-1}$, $702\ cm^{-1}$) > 0	($721\ cm^{-1}$, $702\ cm^{-1}$) = 0	$721\ cm^{-1} = 702\ cm^{-1}$
	($763\ cm^{-1}$, $721\ cm^{-1}$) > 0	($763\ cm^{-1}$, $721\ cm^{-1}$) = 0	$763\ cm^{-1} = 721\ cm^{-1}$
	($2962\ cm^{-1}$, $702\ cm^{-1}$) > 0	($2962\ cm^{-1}$, $702\ cm^{-1}$) = 0	$2962\ cm^{-1} = 702\ cm^{-1}$
	($2962\ cm^{-1}$, $721\ cm^{-1}$) > 0	($2962\ cm^{-1}$, $721\ cm^{-1}$) = 0	$2962\ cm^{-1} = 721\ cm^{-1}$
ODT	($763\ cm^{-1}$, $702\ cm^{-1}$) > 0	($763\ cm^{-1}$, $702\ cm^{-1}$) = 0	$763\ cm^{-1} = 702\ cm^{-1}$
	($721\ cm^{-1}$, $702\ cm^{-1}$) > 0	($721\ cm^{-1}$, $702\ cm^{-1}$) > 0	$721\ cm^{-1} \rightarrow 702\ cm^{-1}$
	($763\ cm^{-1}$, $721\ cm^{-1}$) > 0	($763\ cm^{-1}$, $721\ cm^{-1}$) < 0	$763\ cm^{-1} \leftarrow 721\ cm^{-1}$
	($2962\ cm^{-1}$, $702\ cm^{-1}$) > 0	($2962\ cm^{-1}$, $702\ cm^{-1}$) = 0	$2962\ cm^{-1} = 702\ cm^{-1}$
	($2962\ cm^{-1}$, $721\ cm^{-1}$) > 0	($2962\ cm^{-1}$, $721\ cm^{-1}$) < 0	$2962\ cm^{-1} \leftarrow 721\ cm^{-1}$

the temperature point at 140 °C is only the viscous flow temperature of the main chains of the S blocks. In Fig. 3 around 152 °C, the bands at 2923 cm^{-1}, 2852 cm^{-1}, 763 cm^{-1}, 721 cm^{-1}, and 702 cm^{-1}, which are assigned to the EB and S blocks, show the correlation intensity peaks. This result is consistent with the behaviors of SEBS during the transitions [30]. This temperature point is probably the OOT temperature. However, in this study, the value of 140 °C was so close to that of reported by Krishnamoorti et al. (135–141 °C). Which temperature is the actual OOT temperature? To validate, we employed the atomic force microscopy (AFM) to explore the surface morphology of SEBS.

Fig. 4(a) and (b) shows the surface morphology of the as-prepared SEBS film of samples **1** and **2**, respectively. As shown in Fig. 4(a), sample **1** clearly shows the existence of the cylindrical and spherical microdomains at 140 °C with "worm like" cylinders and spheres of S blocks. However, in sample **2** (Fig. 6(b)), it almost displays spherical microdomains with S block (PS) spheres. It was noticed the pattern state of the PS spheres was a typical body-centered cubic (BCC) sphere morphology. This result is consistent with the work reported before [31–33]. Therefore, we unambiguously assigned 152 °C as the cylinder-to-sphere order–order transition (OOT) temperature of SEBS.

However, something should be discussed in detail. It was reported that the OOT of the block copolymers (SBS, SIS, and SEBS) was very slow (24–72 h) using the annealing experiment [13,31,32]. However, if the block copolymers samples were shear-aligned before the measurement [33,62,63], the time spent by the OOT will become very fast, since the S blocks could form perfect cylinders. In our experiment, the SEBS film sample on the KBr disk was cast from the cyclohexane solution and it was dried only 240 min at 90 °C. The total heating time (20–90 °C → 90 °C → 90–152 °C) was only 36.4 min. No other treatment was employed before the IR measurement. Why the MW2D method can determine the OOT of the SEBS within a short time in this study? We think it may be explained as follows. In our studies, the SEBS thin film samples were cast from the dilute solution and the film thickness on the KBr disk was within 25 μm. But the SEBS samples reported before were direct prepared from heating pressing in a Carver press or cast from a concentrated solution with about 1–2 mm thickness. In the present study, a fraction of the S blocks probably form the relatively perfect PS cylinders during the casting from the diluted solution. The OOT time spent by these relatively perfect PS cylinders is very short. Thus, we can easily observe the OOT around 152 °C from Fig. 3. This finding is similar with the reported by Kim et al. [62] In their paper, it was found the OOT of SIS can be easily determined by DSC of ultrahigh sensitivity. The fastest heating rate in their study was 20 °C/min. It is much faster than the one used in this study (5 °C/min). This viewpoint can also be used to explain why there still has a few PS "worm" do not complete the OOT at 152 °C in the AFM image (Fig. 4(b), the small arrows mark the position of some PS "worm"). Some research groups defined the OOT time as the time that all the PS cylinders (perfect and imperfect) complete the cylinder-to-sphere transition, and therefore the long annealing time is necessary.

As mentioned at the beginning of this section, the bands at 2962 cm^{-1} show no correlation intensity peak. The bands at 2962 cm^{-1} were assigned to the C–H asymmetry stretching vibration of the $-CH_3$ of the ethyl branches in the EB blocks. It may be due to the correlation intensity at 2962 cm^{-1} is very small, so it is not revealed by Fig. 3(a). To gain the mechanism of the OOT of SEBS, the generalized 2D correlation analysis was performed with the dynamic IR spectra within the OOT temperature range. As shown in

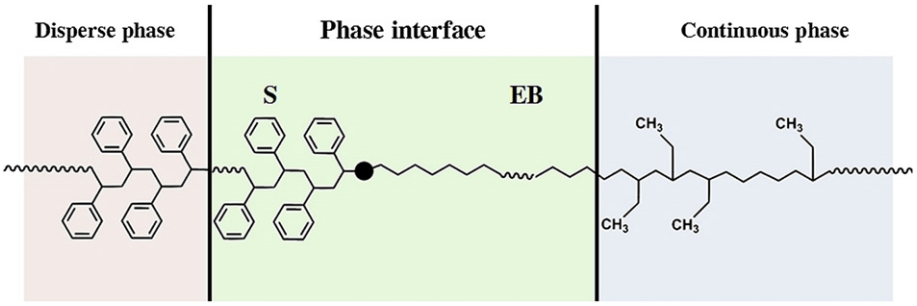

Fig. 7. Sketch of SEBS and the ambient temperature is above 150 °C. The center area between two vertical heavy lines is the phase interface. The solid round dot stands for chemical joint between polystyrene and poly(ethylene-*co*-1-butene). The molecular structure of EB blocks which is close to the chemical joint is almost the $-CH_2-$ and little ethyl branches exist within the interface.

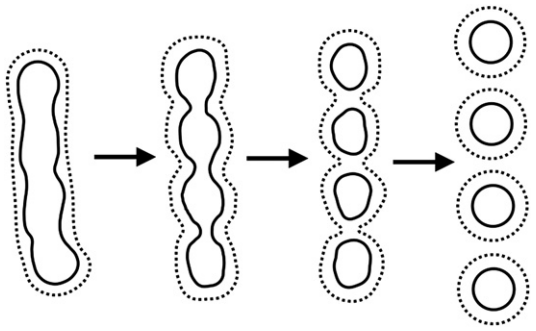

Fig. 8. Whole process of polystyrene cylinders transiting to the spheres, around 152 °C. The area between the solid lines and dashed lines represents the phase interface.

Fig. 3, the range of A which is 145–164 °C is defined as the OOT temperature range. The synchronous and asynchronous IR spectra in 780–680 cm^{-1} are shown in Fig. 5. The small crosses mark the precise positions at (763 cm^{-1}, 702 cm^{-1}), (721 cm^{-1}, 702 cm^{-1}), and (763 cm^{-1}, 721 cm^{-1}). The synchronous and asynchronous IR spectra between 780–680 cm^{-1} and 3000–2800 cm^{-1} are shown

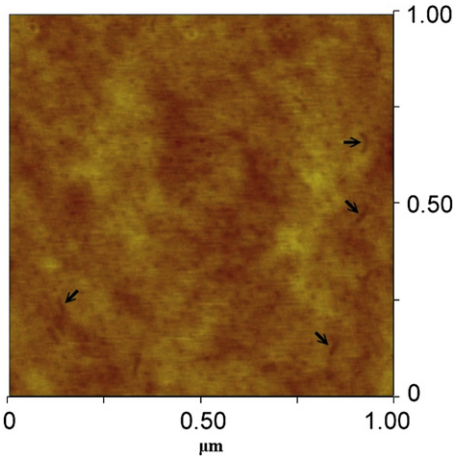

Fig. 9. AFM height images (1 × 1 μm) showing the surface morphology of SEBS films on mica flakes. The SEBS film was prepared through rapid quenching with freezing absolute ethyl alcohol at 170 °C. The small arrows show the position of some PS "worm".

in Fig. 6. The results are listed in Table 2. According to Noda's rules, the movement of $-CH_2-$ of the main chains in the EB blocks is before that of benzene ring in S blocks, as well as before that of $-CH_3$ in EB blocks. This shows the key driver of the OOT is the movements of $-CH_2-$ in the main chains of the EB blocks. In fact [34], there is a thick phase interface between the EB and S blocks at this high temperature (152 °C). Since the interface is a transitional region, the molecular chains of the S and EB blocks coexist. Because of the process of SEBS synthesis, a small mount of the EB blocks, which connects with the chemical joints, is mostly the $-CH_2-$. That is to say, the molecular structure of the EB blocks contains all $-CH_2-$ and there are no ethyl branches within the interface (Fig. 7). As shown in Fig. 8, during the OOT, the S blocks is encapsulated by the interface, which can explain why $-CH_2-$ is the key driver.

As reported by Krishnamoorti et al. [31–33], the OOT of SEBS can be conveniently detected using SANS, rheological measurements, and TEM. In SANS, for example, near the OOT the characteristic of the q ratios was fully different and the q position of the primary peak was shifted largely when the temperature was raised. The microstructure transformation of OOT was monitored by SANS and rheological measurements, but the structural assignments were still unclear. So TEM experiments were performed to determine the structural change during the OOT. In this study, MW2D is sensitive to OOT of SEBS. The structural assignments of OOT were aided by AFM. The morphology in our AFM images (Fig. 4) is very similar with that of TEM pictures in Krishnamoorti's papers. Although SANS, rheological measurements, and TEM can gain the transition temperature and the morphology change of OOT, these methods have no capacity to gain the mechanism from functional groups. MW2D combined generalized 2D correlation spectroscopy not only detected the OOT with high sensitivity, but also gain the sequential order of functional groups movements of SEBS during OOT.

4.3. Lattice disordering transition

In Fig. 3, it can be determined the LDT temperature around 170 °C. There are five weak correlation intensity peaks appear around 170 °C. The corresponding bands assignments are listed in Table 1. According to the literature [26], the lattice disordering transition (LDT) temperature was always between the OOT and the ODT. We speculate 170 °C is the lattice disordering transition (LDT) temperature of G1657.

AFM measurement was also employed to explore the surface morphology transition of the SEBS at 170 °C. Fig. 9 shows the surface morphology of the as-prepared SEBS film samples **3**. It shows the

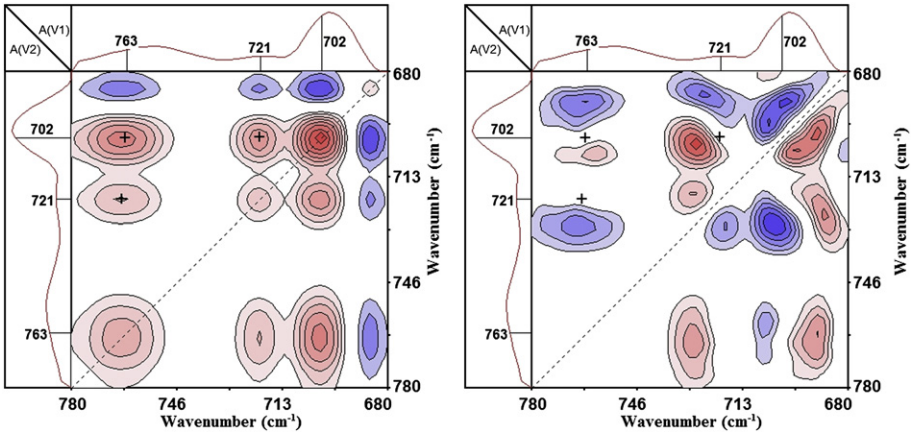

Fig. 10. Synchronous and asynchronous IR spectra of the LDT (164–187 °C) in 780–680 cm^{-1}. The small crosses mark the precise position at (763 cm^{-1}, 702 cm^{-1}), (721 cm^{-1}, 702 cm^{-1}), and (763 cm^{-1}, 721 cm^{-1}).

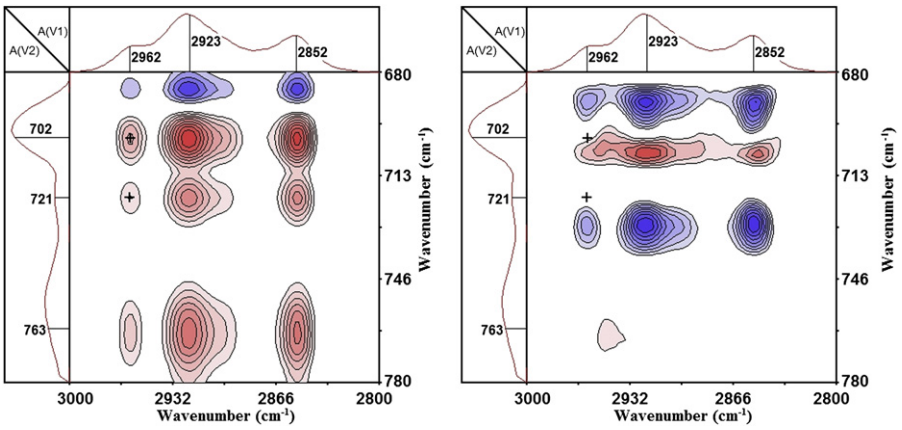

Fig. 11. Synchronous and asynchronous IR spectra of the LDT (164–187 °C) between 780–680 cm^{-1} and 3000–2800 cm^{-1}. The small crosses mark the precise position at (2962 cm^{-1}, 702 cm^{-1}) and (2962 cm^{-1}, 721 cm^{-1}).

disorder spheres of the S blocks. However at 152 °C (Fig. 4(b)), it was a typical body-centered cubic (BCC) sphere morphology. It solidified that the temperature determined by MW2D around 170 °C was indeed the LDT of the SEBS. It should be noticed there still had a small mount of PS "worm" exist at 170 °C, such as the "worm" mentioned in Fig. 4(b). It suggested the imperfect PS spent longer time to complete the OOT. The OOT of these imperfect PS will not finish at all within a short thermal treatment time, even though the environment temperature (170 °C) is higher than the OOT temperature (152 °C). It can be concluded that the PS "worm" will direct involve in the order–disorder transition (ODT) with the temperature increasing in further.

It is also noticed the bands at 2962 cm^{-1} show no correlation intensity peak around 170 °C (Fig. 3). It also may be due to the correlation intensity at 2962 cm^{-1} is very small, so it is not revealed. The dynamic IR spectra within the LDT temperature range were analyzed using the generalized 2D correlation method. The range of B which is 164–187 °C is defined as the LDT temperature range in Fig. 3. The synchronous and asynchronous IR spectra in 780–680 cm^{-1} are shown in Fig. 10. The small crosses mark the precise positions at (763 cm^{-1}, 702 cm^{-1}), (721 cm^{-1}, 702 cm^{-1}), and (763 cm^{-1}, 721 cm^{-1}). The synchronous and asynchronous IR spectra between 780–680 cm^{-1} and 3000–2800 cm^{-1} are shown in Fig. 11. The results are listed in Table 2. According to Noda's rules, $-CH_2-$ (EB blocks) = benzene ring (S blocks) = $-CH_3$ (EB blocks). The movements of these groups are simultaneous. It is proved the SEBS molecular chains move as a whole in the LDT. The process may be described as follows. G1657 shows a body-centered cubic (BCC) sphere morphology between 152 °C and 170 °C; meanwhile, the PS spheres are at the equilibrium position. There are already a fraction of the polystyrene chains enter the interface when the temperature is below 170 °C. As the temperature increases above 170 °C, these polystyrene chains suddenly escape from the interface and then enter the EB blocks. Because of the unbalanced force around the PS spheres, the PS spheres quickly deviate from the equilibrium position, which leads to the LDT (Fig. 12).

Kim et al. [26] studied the LDT of a highly asymmetric SEBS with a volume fraction of PS of 0.084. On the basis of SAXS, TEM, and rheological measurements, the LDT of SEBS was successfully determined. In SAXS, the higher order diffraction peaks from the BCC structure disappeared above the LDT temperature. The particle scattering of spheres due to the intraparticle or interparticle interference was clearly observed between the LDT and ODT. It was also found that a precipitous decrease in storage modulus (G') in rheological measurements and a change in morphology of TEM occurred at the same temperature of the LDT. However, in Krishnamoorti's [31–33] paper, the LDT of SEBS was not detected. The SEBS sample used by Krishnamoorti et al. is the same as this study. It indicates that the sensitivity of measurements employed by Krishnamoorti et al. is far lower than MW2D and it's hard to detect the LDT clearly. In this study, MW2D conveniently determines the LDT without difficulties. The sequential order of functional groups movements of SEBS during LDT is well understood using generalized 2D correlation analysis.

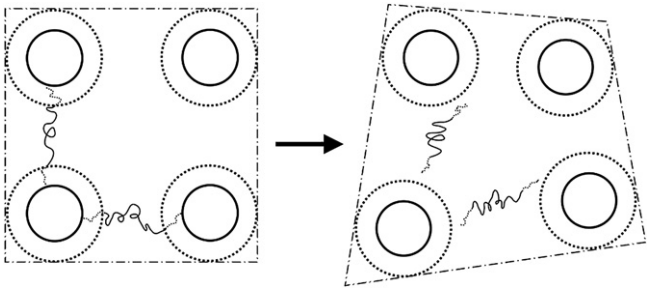

Fig. 12. Sketch of the mechanism of the SEBS LDT. The area between the solid circles and the dashed circles represents the phase interface. The thin solid lines and the thin dashed lines represent the molecular chains of EB and S blocks, respectively.

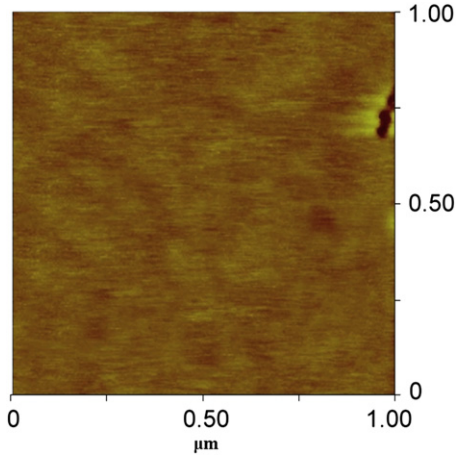

Fig. 13. AFM height images (1 × 1 μm) showing the surface morphology of SEBS films on mica flakes. The SEBS film was rapid quenched in freezing absolute ethyl alcohol at 202 °C.

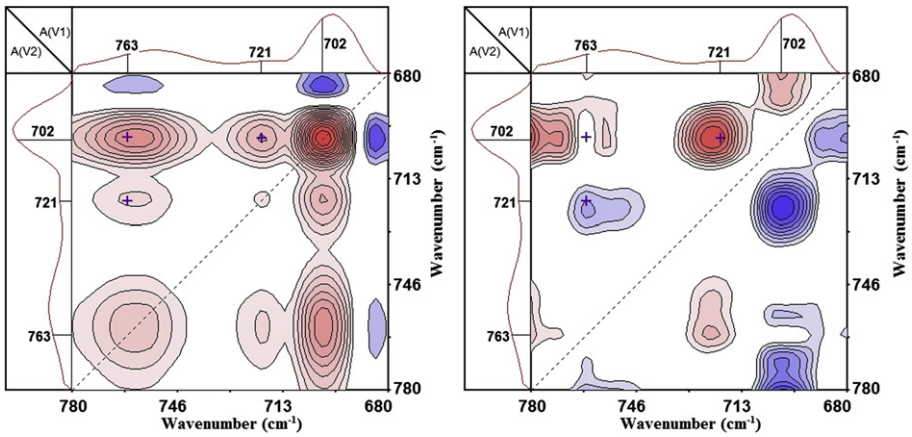

Fig. 14. Synchronous and asynchronous IR spectra of the ODT (194–210 °C) in 780–680 cm^{-1}. The small crosses mark the precise position at (763 cm^{-1}, 702 cm^{-1}), (721 cm^{-1}, 702 cm^{-1}), and (763 cm^{-1}, 721 cm^{-1}).

4.4. Order–disorder transition

As shown in Fig. 3, several strong correlation intensity peaks appear around 202 °C. All the spectral bands of the SEBS (S and EB blocks) show correlation intensity. It is obviously an outcome of the order–disorder transition (ODT) of SEBS. Many researchers [9,19–21,31] studied the ODT of the block copolymers. When the temperature reached the ODT temperature, the interaction parameter (χ) between the blocks became zero. The ODT was the transition that the molecular chains of the different blocks underwent interpenetration. Therefore, the final result of the ODT was to achieve the uniform polymer bulk in block copolymers. Moreover, when the temperature was higher than the ODT temperature, the microphase separation of the block copolymers vanished. Unlike the OOT, the speed of the complete ODT of the block copolymers was very fast. Krishnamoorti et al. [31,32] reported the order–disorder transition (ODT) of the SEBS (G1657) was about 200 °C. This result is almost the same as determined by MW2D in this study.

Fig. 13 shows the surface morphology of the as-prepared SEBS film samples **4**. It clearly shows the microphase separation of the SEBS disappears entirely. The dynamic IR spectra within the ODT temperature range were also analyzed using the generalized 2D correlation method. The range of C (194–210 °C) is defined as the ODT temperature range in Fig. 3. The synchronous and asynchronous spectra in 780–680 cm^{-1} are shown in Fig. 14. The synchronous and asynchronous IR spectra between 780–680 cm^{-1} and 3000–2800 cm^{-1} are shown in Fig. 15. The results are listed in Table 2. According to Noda's rules, $-CH_2-$ (EB blocks) → $-CH_3$ (EB blocks) and $-CH_2-$ (EB blocks) → benzene ring (S blocks). This shows the driver of the ODT is the movements of $-CH_2-$ in the main chains of the EB blocks. The process of the ODT is the infiltration of $-CH_2-$ (EB blocks) in S blocks.

SANS, SAXS, and rheological measurements were the classic methods to detect the ODT of SEBS [26,31–33]. In rheological measurements, the ODT is defined by the temperature where the storage modulus G' drops precipitously. In plots of logG' versus logG'', the ODT is also taken as the threshold temperature, above which these plots are independent of temperature. In Kim and Krishnamoorti's [26,31–33] papers, none of TEM pictures above ODT temperature was provided. In contrast, Fig. 13 clearly illustrates the vanishing of the SEBS structures. Although SANS, SAXS, and rheological measurements can determined ODT clearly, the process of ODT with functional groups is not available. In general, scientists considered the ODT of SEBS was the transition caused by inter-diffusion between EB and S blocks. In this study, the detail mechanism of the ODT process which is interpreted from functional groups level is gained using MW2D combined with generalized 2D analysis. From the sequential order of the functional groups, it can be easily gained that the movements of groups of EB

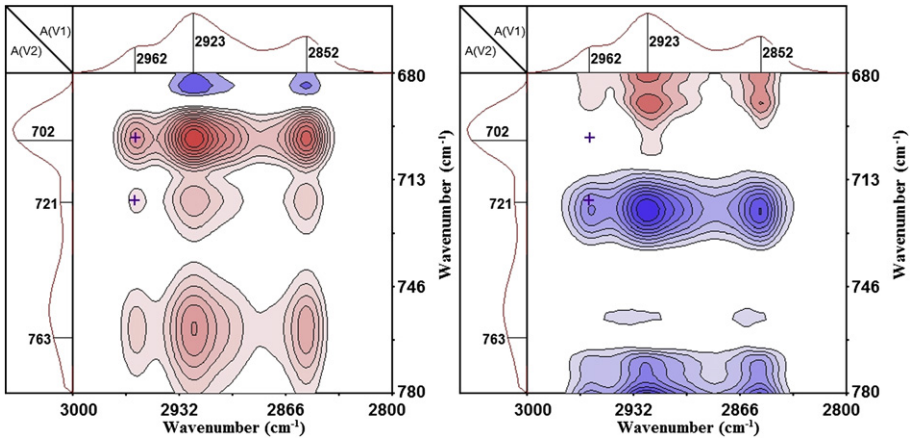

Fig. 15. Synchronous and asynchronous IR spectra of the ODT (194–210 °C) between 780–680 cm^{-1} and 3000–2800 cm^{-1}. The small crosses mark the precise position at (2962 cm^{-1}, 702 cm^{-1}) and (2962 cm^{-1}, 721 cm^{-1}).

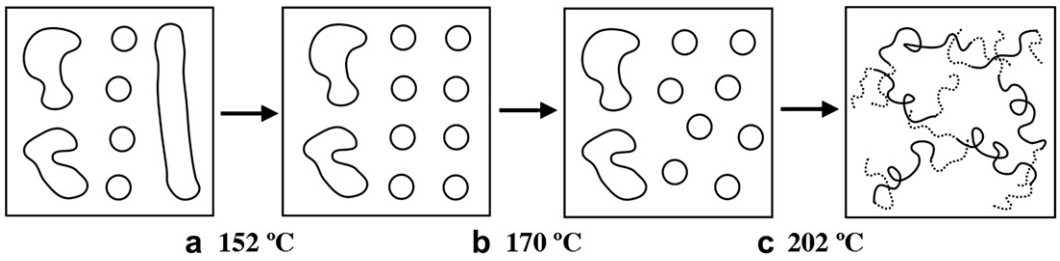

Fig. 16. Transitions revealed in this paper. (a) The OOT, around 152 °C. The rapid transition of the relatively perfect PS cylinders to the spheres. While the PS "worm" still keep the shape during the transition; (b) the LDT, around 170 °C. The PS "worm" still retains its shape during the transition. (c) The ODT, around 202 °C. The PS "worm" direct involves in the ODT.

blocks are apparently before that of S blocks during the ODT. So the mechanism of ODT of SEBS is probably caused by infiltration of EB blocks into the domains of S blocks. In Fig. 16, it draws the transitions revealed in the present study.

5. Conclusion

In the present study, the two-dimensional correlation spectroscopy was employed to study the temperature-dependent IR of SEBS at high temperature. The order–order transition, the lattice disordering transition, and the order–disorder transition of SEBS were revealed with a linear temperature increment ranging from 100 °C to 220 °C.

(1) 152 °C, the cylinder-to-sphere order–order transition.
(2) 170 °C, the lattice disordering transition.
(3) 202 °C, the order–disorder transition.

The order–order transition, the lattice disordering transition and the order–disorder transition of block copolymers can be conveniently determined by MW2D. As everyone knows, the investigated subject of MW2D correlation spectroscopy is microscopic and submicroscopic molecular movements. In our study, these microscopic or submicroscopic molecular movements can be used to explain the meso transitions through IR combined with MW2D. From the results of generalized 2D correlation infrared spectroscopy, it gained the mechanism of OOT, LDT, and ODT in functional group level. The key driver of the OOT is the movements of $-CH_2-$ in the main chains of the EB blocks. In the LDT, the movements of groups are simultaneous and the SEBS molecular chains move as a whole. In the ODT, it shows that the driver is the movements of $-CH_2-$ in the main chains of the EB blocks. The process of the ODT is the infiltration of $-CH_2-$ (EB blocks) in S blocks.

Acknowledgments

This work was supported by the National Natural Science Foundation of China (Grant No. 50873071) and the State Key Program of National Natural Science of China (Grant No. 50933004). This work was also supported by the Young Scholars Foundation of Sichuan University (Grant No. 2008017) and the SEBS Microstructure Optimization Project (J404003, 05H238) of Baling Petrochemical Industry Co., Ltd of Sinopec.

References

[1] Holden G, Legge NR, Quirk R, Schroeder HE. Thermoplastic elastomers. 2nd ed. Munich: Hanser; 1996.
[2] Matsen MW, Bates FS. Macromolecules 1996;29(4):1091–8.
[3] Motomatsu M, Mizutani W, Tokumoto H. Polymer 1997;38(8):1779–85.
[4] Matsen MW. J Chem Phys 1998;108(2):785–96.
[5] Khandpur AK, Forster S, Bates FS, Hamley IW, Ryan AJ, Bras W, et al. Macromolecules 1995;28(26):8796–806.
[6] Bondzic S, Polushkin E, Ruokolainen J, ten Brinke G. Polymer 2008;49(11):2669–77.
[7] Jeong U, Lee HH, Yang LH, Kim JK, Okamoto S, Aida S, et al. Macromolecules 2003;36(5):1685–93.
[8] Zhao Y, Saijo K, Takenaka M, Koizumi S, Hashimoto T. Polymer 2009;50(12):2696–705.
[9] Sakamoto N, Hashimoto T, Han CD, Kim D, Vaidya NY. Macromolecules 1997;30(6):1621–32.
[10] Lai CJ, Loo YL, Register RA, Adamson DH. Macromolecules 2005;38(16):7098–104.
[11] Rodriguez-Hidalgo MD, Soto-Figueroa C, Martinez-Magadan JM, Vicente L. Polymer 2009;50(19):4596–601.
[12] Zha WB, Han CD, Lee DH, Han SH, Kim JK, Kang JH, et al. Macromolecules 2007;40(6):2109–19.
[13] Bailey TS, Pham HD, Bates FS. Macromolecules 2001;34(20):6994–7008.
[14] Wang CY, Lodge TP. Macromolecules 2002;35(18):6997–7006.
[15] Sota N, Sakamoto N, Saijo K, Hashimoto T. Macromolecules 2003;36(12):4534–43.
[16] Park MJ, Bang J, Harada T, Char K, Lodge TP. Macromolecules 2004;37(24):9064–75.
[17] Huang YY, Hsu JY, Chen HL, Hashimoto T. Macromolecules 2007;40(10):3700–7.
[18] Arceo A, Green PF. J Phys Chem B 2005;109(15):6958–62.
[19] Spatz JP, Eibeck P, Mossmer S, Moller M, Kramarenko EY, Khalatur PG, et al. Macromolecules 2000;33(1):150–7.
[20] Lynd NA, Hillmyer MA. Macromolecules 2007;40(22):8050–5.
[21] Mita K, Tanaka H, Saijo K, Takenaka M, Hashimoto T. Polymer 2008;49(23):5146–57.
[22] Matsen MW, Bates FS. J Chem Phys 1997;106(6):2436–48.
[23] Hashimoto T, Shibayama M, Kawai H, Watanabe H, Kotaka T. Macromolecules 1983;16:361–71.
[24] Sakamoto N, Hashimoto T, Han CD, Kim D, Vaidya NY. Macromolecules 1997;30(18):5321–30.
[25] Sakamoto N, Hashimoto T. Macromolecules 1998;31(24):8493–502.
[26] Kim JK, Lee HH, Sakurai S, Aida S, Masamoto J, Nomura S, et al. Macromolecules 1999;32(20):6707–17.
[27] Walker BM, Rader CP. Handbook of thermoplastic elastomers. 2nd ed. New York: Van Nostrand Reinhold; 1988.
[28] Xu ZW, Liang YC, Dong S, Cao YZ, Zhao TQ, Wang JH, et al. Ultramicroscopy 2005;105(1–4):72–8.
[29] Han X, Hu J, Liu HL, Hu Y. Langmuir 2006;22(7):3428–33.
[30] Wang L, Hong S, Hu HQ, Zhao J, Han CC. Langmuir 2007;23(5):2304–7.
[31] Modi MA, Krishnamoorti R, Tse MF, Wang HC. Macromolecules 1999;32(12):4088–97.
[32] Krishnamoorti R, Modi MA, Tse MF, Wang HC. Macromolecules 2000;33(10):3810–7.
[33] Krishnamoorti R, Silva AS, Modi MA, Hammouda B. Macromolecules 2000;33(10):3803–9.
[34] Zhou T, Zhang A, Zhao CS, Liang HW, Wu ZY, Xia JK. Macromolecules 2007;40(25):9009–17.
[35] Thomas M, Richardson HH. Vib Spectrosc 2000;24(1):137–46.
[36] Noda I, Dowrey AE, Marcott C, Story GM, Ozaki Y. Appl Spectrosc 2000;54(7):236a–48a.
[37] Noda I, Ozaki Y. Two-dimensional correlation spectroscopy – applications in vibrational and optical spectroscopy. Chichester: John Wiley & Sons; 2004. pp. 15–43.
[38] Li L, Wu Q, Li S, Wu P. Appl Spectrosc 2008;62(10):1129–36.
[39] Meng S, Sun BJ, Guo Z, Zhong W, Du QG, Wu PY. Polymer 2008;49(11):2738–44.
[40] Peng Y, Wu PY. Polymer 2004;45(15):5295–9.
[41] Watanabe S, Noda I, Hu Y, Ozaki Y. Polymer 2007;48(22):6632–8.
[42] Wu YQ, Meersman F, Ozaki Y. Macromolecules 2006;39(3):1182–8.
[43] Yang HX, Sun M, Zhou P. Polymer 2009;50(6):1533–40.
[44] Yu J, Wu PY. Polymer 2007;48(12):3477–85.
[45] Noda I. Appl Spectrosc 1993;47(9):1329–36.
[46] Morita S, Shinzawa H, Tsenkova R, Noda I, Ozaki Y. J Mol Struct 2006;799(1–3):111–20.
[47] Shinzawa H, Morita S, Noda I, Ozaki Y. J Mol Struct 2006;799(1–3):28–33.

[48] Morita S, Shinzawa H, Noda I, Ozaki Y. J Mol Struct 2006;799(1–3):16–22.
[49] Sasic S, Katsumoto Y, Sato N, Ozaki Y. Anal Chem 2003;75(16):4010–8.
[50] Lai HJ, Wu PY. Polymer 2010;51(6):1404–12.
[51] Morita S, Kitagawa K, Noda I, Ozaki Y. J Mol Struct 2008;883:181–6.
[52] Morita S, Shinzawa H, Noda I, Ozaki Y. Appl Spectrosc 2006;60(4):398–406.
[53] Sun S, Tang H, Wu P, Wan X. Phys Chem Chem Phys 2009;11(42):9861–70.
[54] Unger M, Morita S, Sato H, Ozaki Y, Siesler HW. Appl Spectrosc 2009;63 (9):1027–33.
[55] Unger M, Morita S, Sato H, Ozaki Y, Siesler HW. Appl Spectrosc 2009;63 (9):1034–40.
[56] Holland-Moritz K, Sausen E. J Polym Sci Polym Phys 1979;17(1):1–23.
[57] Ishioka T, Wakisaka H, Kanesaka I, Nishimura M, Fukasawa H. Polymer 1997;38(10):2421–30.
[58] Sharma P, Tandon P, Gupta VD. Eur Polym J 2000;36(12):2629–38.
[59] Krimm S. Adv Polym Sci 1960;2:51–172.
[60] Naka Y, Nemoto N, Song Y. J Polym Sci B Polym Phys 2005;43(12):1520–31.
[61] Sworen JC, Smith JA, Berg JM, Wagener KB. J Am Chem Soc 2004;126(36): 11238–46.
[62] Kim JK, Lee HH, Gu QJ, Chang TH, Jeong YH. Macromolecules 1998;31(12): 4045–8.
[63] Koppi KA, Tirrell M, Bates FS, Almdal K, Mortensen K. J Rheol 1994;38: 999–1027.